Singular points, squeezing, and nonadiabatic transitions in the dressed-atom Jaynes-Cummings model

Georgii P. Miroshnichenko*
Department of Mathematics, St. Petersburg State Institute of Fine Mechanics and Optics, 14 Sablinskaya Str., St. Petersburg 197101, Russia

Michael Z. Smirnov†
Department of Quantum Electronics and Biomedical Optics, St. Petersburg State Institute of Fine Mechanics and Optics, 14 Sablinskaya Str., St. Petersburg 197101, Russia

(Received 14 May 2001; published 27 September 2001)

We study the quasienergy spectrum and the nonadiabatic time dynamics of the open quantum system, which incorporates the two-level atom dipole coupled to both the quantized mode and the polychromatic classical field. Both the numeric calculations and the original perturbation technique are applied to track the quasilevel positions against the strength of the classical field. The first-order perturbation theory predicts the singular behavior of the system including the infinitely large squeezing of the quantized mode quadratures at certain values of the field strength. The singularity is removed here by allowing for the nonadiabatic transitions among the quasienergy states and the higher perturbations as well.

DOI: 10.1103/PhysRevA.64.053801 PACS number(s): 42.50.Dv, 42.50.Ct, 42.50.Hz

I. INTRODUCTION

The recent progress in the technology of trapped-atom lasers and the cavity QED experiments [1–5] has resumed the interest of researchers in the single-atom Jaynes-Cummings (JCM) model [6], the multiatom Tavis-Cummings model (TCM) [7], and the modifications of these basic models as well. One may use, particularly, the superconductive high-Q cavity to reach the strong coupling regime of the atom and cavity mode, with the cavity decay rate being much smaller than the coupling constant between the atom and the mode [4]. This makes it possible for a photon to be absorbed and reemitted by the atom repeatedly before it escapes the cavity. In this way, the experimentalists have observed some nontrivial effects predicted for the JCM. These include, in particular, the collapses and revivals of atomic inversion [5], the coupling-induced normal-mode splitting [4], the squeezed-light generation [8], the macroscopic superposition of states (Schrödinger cat states) [9], the Fock states of the quantized mode [10], the correlated atom-field states [2], etc. A detailed review on this topic may be found in Refs. [1] and [2].

The solutions obtained for the models in question may be considered in the context of other issues. A particular example is the theory of laser cooling of trapped atoms and ions. Reference [11] demonstrates here that the JCM Hamiltonian may describe the interaction between the translational and internal degrees of freedom of a driven atom in a trap in the Lamb-Dicke limit. In this context, the boson operators describe the confined translational motion and the quantized field effects, those found earlier for the conventional JCM gain a different meaning thereof. In this way, various nonclassical states of ion motion have been predicted theoretically and observed experimentally, for instance, Fock states, Schrödinger cat states, even and odd coherent states, etc. More detailed information on this matter may be found in Refs. [12].

The nonclassical states of the electromagnetic field and those of the confined movement of trapped atoms, as well, have found various applications including nondemolition measurements [13]. A field of research called in [14] the quantum state engineering deals with generation schemes for the predefined quantum states. These schemes are based, as a rule, on the JCM generalizations. It seems, therefore that the externally driven (open) JCM and TCM may be subjects of special interest.

The first studies of the open models of this kind have demonstrated a number of interesting phenomena. For instance, using an external classical field to drive the JCM provides a means for obtaining some nonclassical states of light with predefined characteristics [14]. To get the information on the dynamics of the driven JCM, one may measure the spectrum of the resonance fluorescence [15].

The authors of Ref. [16] have found the eigenvectors and the corresponding eigenvalues of the modified JCM, where either the atom or the cavity mode is coupled to the external monochromatic classical field with the carrier frequency coinciding to that of the cavity mode. In the case of the driven atom, it was demonstrated that the eigenvectors of this model are the properly shifted eigenvectors of the conventional JCM, while the eigenvalues of both models are the same. The derivation above means, in essence, that one can remove the driving field from the model by incorporating it into the cavity field of the same carrier frequency. In the case of the driven cavity mode, the results of Ref. [16] are somewhat more interesting. The eigenvectors are found to be the direct products of the special states of the atom and the squeezed number states of the cavity mode with the degree of squeez-

*Electronic address: mirosh@mkk.ifmo.ru
†Electronic address: mz_smirnov@mailru.com; FAX: 7(812)315-71-33

ing depending on the strength of the classical field.

A more general JCM modification called the dressed-atom Jaynes-Cummings model (DAJCM) was introduced in Refs. [17]. This model includes the polychromatic (periodically modulated) classical field coupled to the atom. The eigenvectors of the model Hamiltonian obtained within the second RWA appeared to be the bilinear combinations of the quasienergy (Floquet) states of the dressed atom and the squeezed number states of the mode [18]. The most interesting feature of the DAJCM, which is not a property of the other known JCM modifications, is the presence of singular points at certain values of both the amplitude and the modulation frequency of the driving field. At these points, the degree of squeezing of the cavity mode tends to infinity, while the eigenvalue spectrum becomes continuous.

In this paper, we present the theory of the DAJCM based on the quasienergy approach. This theory also applies to the multiatom case. We develop the perturbation technique to find the quasienergy operator of the DAJCM. The first-order quasienergy operator coincides hereby with the effective DAJCM Hamiltonian of Refs. [17] derived from the second RWA. However, to explain some interesting features of the quasienergy diagram that were calculated numerically, one needs at least the third-order perturbation technique. Then, we describe the possible method of squeezing the quadratures of the cavity mode and analyze the basic limitations on the squeezing degree result from the nonadiabatic transitions among the quasienergy states and from the higher-order perturbation terms as well.

The organization of the paper is as follows: Section II develops the perturbation technique for the Schrödinger equation with time-periodic Hamiltonian. Section III presents the quasienergy approach to the theory of DAJCM, including the case of many atoms. The subsequent considerations are restricted to the case of single atom and bichromatic driving field. Section IV compares the quasienergy diagrams calculated numerically with those obtained using the first- and third-order perturbation techniques. The nonadiabatic effect appearing at the change of the driving field strength is studied in Sec. V, using the first-order perturbation technique. Finally, Sec. VI outlines the major results of the paper.

II. PERTURBATION THEORY FOR THE QUASIENERGY OPERATOR

In this section we give a brief summary on the Schrödinger equation with time-periodic Hamiltonian given by

$$\frac{d}{dt}|\psi(t)\rangle = -i\mathbf{H}(t)|\psi(t)\rangle; \quad \mathbf{H}(t+T)=\mathbf{H}(t). \tag{2.1}$$

Then, we develop a perturbation technique to find the quasienergy operator of a quantum system driven by a time-periodic external force.

The solution to Eq. (2.1) may be expressed in terms of time-evolution operator $\mathbf{U}(t)$

$$|\psi(t)\rangle = \mathbf{U}(t)|\psi(0)\rangle. \tag{2.2}$$

The latter operator, in its turn, is determined by the following equations:

$$i\frac{d}{dt}\mathbf{U}(t)=\mathbf{H}(t)\cdot\mathbf{U}(t); \quad \mathbf{U}(0)=\mathbf{I}; \quad \mathbf{U}^{\dagger}\mathbf{U}=\mathbf{U}\cdot\mathbf{U}^{\dagger}=\mathbf{I}, \tag{2.3}$$

with $\mathbf{I}$ being the identity operator. Based on the Floquet theorem [19], the solution to Eqs. (2.3) may be chosen in the following general form:

$$\mathbf{U}(t)=\mathbf{u}(t)\exp(-i\,\mathbf{Q}\,t); \quad \mathbf{u}(0)=\mathbf{I}; \quad \mathbf{u}(t+T)=\mathbf{u}(t), \tag{2.4}$$

with $\mathbf{Q}$ and $\mathbf{u}(t)$ being the time-independent (Hermitian) quasienergy operator and a time-periodic unitary operator, respectively. It should be noted here that the quasienergy operator is determined ambiguously. Actually, one may augment each eigenvalue of this operator by a multiple of the modulation frequency $\omega_{\mathrm{M}}\equiv 2\pi/T$ without violating relations (2.4). Therefore, one may always redistribute the eigenvalues of the quasienergy operator among the Brillouin bands with the interband spacing equal to ω_{M}.

Solution (2.4) gains a particular physical significance if some eigenvalues of quasienergy operator $\mathbf{Q}$ (within the first Brillouin band) are small compared to ω_{M}. If this is the case, the time dynamics of the system branches into the fast and slow oscillations, with the specific time for the fast oscillations being $2\pi/\omega_{\mathrm{M}}$. Simultaneously, the specific time for the slow oscillations is determined by the small eigenvalues mentioned above. If one is interested in the slow oscillations, only the course-grained time scale may be introduced with the grain size being great compared to $2\pi/\omega_{\mathrm{M}}$, but much smaller than the specific time for the slow oscillations. From this point of view one may consider the quasienergy operator as the ''slow Hamiltonian,'' which governs the slow oscillations but neglects the fast oscillations. The slow oscillations are described here in the course-grained time scale.

Now, let Hamiltonian $\mathbf{H}(t)$ be a sum of the two time-periodic terms: the zeroth-order Hamiltonian $\mathbf{H}_0(t)$, and the small perturbation term $\mathbf{V}(t)$

$$\mathbf{H}(t)=\mathbf{H}_0(t)+\mathbf{V}(t),$$
$$\mathbf{H}_0(t+T)=\mathbf{H}_0(t); \quad \mathbf{V}(t+T)=\mathbf{V}(t); \quad |\mathbf{V}|\ll|\mathbf{H}_0|. \tag{2.5}$$

Furthermore, we suggest that the zeroth-order Schrödinger equation with Hamiltonian $\mathbf{H}_0$ may be solved to yield the corresponding quasienergy operator $\mathbf{Q}_0$ and time-periodic operator $\mathbf{u}_0(\mathbf{t})$.

Substituting Eq. (2.4) into Eq. (2.3) and using presentation (2.5) yields the following equation:

$$i\frac{d}{dt}\mathbf{u}+\mathbf{u}\cdot\mathbf{Q}=(\mathbf{H}_0+\mathbf{V})\cdot\mathbf{u}, \tag{2.6}$$

while the zeroth-order operators $\mathbf{Q}_0$ and $\mathbf{u}_0(\mathbf{t})$ obey the same equation, with term $\mathbf{V}$ being eliminated

$$i\frac{d}{dt}\mathbf{u}_0+\mathbf{u}_0\cdot\mathbf{Q}_0=\mathbf{H}_0\cdot\mathbf{u}_0. \tag{2.7}$$

Our aim is to develop the perturbation technique for solving Eq. (2.6). As a first step, we use unitary transform $\mathbf{u}_0(t)$ to get a new time representation referred to here as the time-periodic picture (TP). Within the TP operator, $\mathbf{u}(t)$ is presented as

$$\mathbf{u}(t)\equiv\mathbf{u}_0(t)\cdot\mathbf{W}(t), \tag{2.8}$$

where $\mathbf{W}(t)$ is unitary and time-periodic operator that obeys the initial condition

$$\mathbf{W}(0)=\mathbf{I}. \tag{2.9}$$

Simultaneously, the perturbation Hamiltonian is represented by

$$\mathbf{V_{TP}}(\mathbf{t})=\mathbf{u}_0^{\dagger}(\mathbf{t})\cdot\mathbf{V}(\mathbf{t})\cdot\mathbf{u}_0(\mathbf{t}). \tag{2.10}$$

The equation for operator $\mathbf{W}(t)$ is obtained here in a straightforward manner. Substituting Eq. (2.8) into Eq. (2.6) and using Eq. (2.7), one gets

$$i\frac{d}{dt}\mathbf{W}+\mathbf{W}\cdot\mathbf{Q}=(\mathbf{Q}_0+\mathbf{V_{TP}})\mathbf{W}. \tag{2.11}$$

To simplify the further derivations, let us first replace, temporarily, initial condition (2.9) by the following condition:

$$\mathbf{M}\{\mathbf{W}\}=\mathbf{I}, \tag{2.12}$$

where notation $\mathbf{M}\{\bullet\}$ stands for time averaging of a time-periodic operator over its period, particularly, $\mathbf{M}\{\mathbf{W}\}=T^{-1}\int_0^T\mathbf{W}(t)dt$.

To get the solution of Eq. (2.11) satisfying condition (2.12), one may use various asymptotic methods described elsewhere (see book Ref. [21] for a detailed review). A particular example is a direct expansion of the solution into power series in $\mathbf{V}_{\mathrm{TP}}$ as outlined a shade below. At this point, we suggest that $\mathbf{W(t)}$ is a solution for Eqs. (2.11) and (2.12) obtained in some way. How to get the quasienergy operator $\mathbf{Q}$ from this solution? While averaging both sides of Eq. (2.11) over time interval $T=2(\pi/\omega_{\mathrm{M}})$, one notes that the time derivative of periodic operator $\mathbf{W}$ averages to zero. Then, using condition (2.12) one gets

$$\mathbf{Q}=\mathbf{Q}_0+\mathbf{M}\{\mathbf{V_{TP}}(t)\cdot\mathbf{W}(t)\}. \tag{2.13}$$

It should be noted that Eq. (2.13) does not give us the final result yet, since initial condition (2.12) does not coincide with the true initial condition (2.9). To get the correct quasienergy and time evolution operators, one has to apply the following transform:

$$\mathbf{Q}=\tilde{\mathbf{W}}(0)\cdot\tilde{\mathbf{Q}}\cdot\tilde{\mathbf{W}}(0)^{-1};\quad \mathbf{W}(t)=\tilde{\mathbf{W}}(t)\cdot\tilde{\mathbf{W}}(0)^{-1}, \tag{2.14}$$

where $\tilde{\mathbf{W}}$ and $\tilde{\mathbf{Q}}$ are the solution obeying condition (2.12).

Now, let us return to Eqs. (2.11) and (2.12). As argued above, these two equations yield relation $\mathbf{Q}=\mathbf{Q_0}+\mathbf{M}\{\mathbf{V_{TP}(t)}\cdot\mathbf{W(t)}\}$. Substituting the latter relation into Eq. (2.11) yields the self-consistent equation for operator $\mathbf{W(t)}$

$$i\frac{d\mathbf{W}}{dt}+[\mathbf{W},\mathbf{Q_0}]=\mathbf{V_{TP}}\cdot\mathbf{W}-\mathbf{W}\cdot\mathbf{M}\{\mathbf{V_{TP}}\cdot\mathbf{W}\}, \tag{2.15}$$

where square brackets stand for the commutator, i.e., $[\mathbf{a},\mathbf{b}]\equiv\mathbf{a}\cdot\mathbf{b}-\mathbf{b}\cdot\mathbf{a}$.

We seek for the solution of Eq. (2.15) in the form.

$$\mathbf{W}=\mathbf{W_0}+\mathbf{W_1}+\mathbf{W_2}+\cdots. \tag{2.16}$$

Here, term $\mathbf{W_n}$ is of the **n**th infinitesimal order assuming operator $\mathbf{V_{TP}}$ to be of the first infinitesimal order. Substituting Eq. (2.16) into Eq. (2.15) and equating variables of the same infinitesimal order yields the following set of equations:

$$i\frac{d}{dt}\mathbf{W_0}+[\mathbf{W_0},\mathbf{Q_0}]=0,$$

$$i\frac{d}{dt}\mathbf{W}_j+[\mathbf{W}_j,\mathbf{Q_0}]=\mathbf{V_{TP}}\cdot\mathbf{W_j}-\mathbf{1}-\sum_{n=0}^{j-1}\mathbf{W_{j-n-1}}\cdot\mathbf{M}\times\{\mathbf{V_{TP}}\cdot\mathbf{W_n}\},\quad j=1,2,\ldots. \tag{2.17}$$

One may choose the solution for the first equation of set (2.17) to be $\mathbf{W_0}=\mathbf{I}$. When solving the other equations, the constants of integration should be chosen to meet conditions $\mathbf{M}\{\mathbf{W_j}\}=0,\quad j=1,2,\ldots.$

III. POLICHROMATICALLY DRIVEN SYSTEM OF ATOMS: A QUASIENERGY APPROACH

Now, let us apply the formalism of the previous section to study the dynamics of a system of two-level atoms dipole coupled to the quantized mode of electromagnetic field and to the polychromatic (modulated) electromagnetic field as well. The modulation frequency ω_{M} is assumed to be very small compared to the carrier frequency Ω of the polychromatic field, the quantized field carrier ω, and the atomic transition frequency ω_0. Dropping the fast-oscillating terms, the Hamiltonian of the system reads

$$\mathbf{H}(t)=\omega\mathbf{a}^{\dagger}\cdot\mathbf{a}+\omega_0\mathbf{S}_z+g(t)\exp(-i\,\Omega t)\mathbf{S}_+ +g^*(t)\exp(i\,\Omega t)\mathbf{S}_-+\kappa_{\mathrm{aq}}(\mathbf{S}_+\cdot\mathbf{a}+\mathbf{S}_-\cdot\mathbf{a}^{\dagger}), \tag{3.1}$$

where the first two terms are the Hamiltonians of the unperturbed quantized mode and the unperturbed TLA, respectively, the next couple of terms describes the interaction between the TLA and the polychromatic field, and the last couple of terms are the interaction Hamiltonian between the TLA and the quantized mode. The notations in Eq. (3.1) are as follows: ω is the eigenfrequency of the quantized mode, ω_0 is the atomic transition frequency, $g(t)$ is the strength of

the polychromatic field assumed to be a periodic function of time with period $T=2\pi/\omega_M$, κ_q is the coupling constant between the atom and the quantized mode, $\mathbf{a}$ and $\mathbf{a}^\dagger$ are the annihilation and creation operators of the quantized mode, $\mathbf{S}_+$, $\mathbf{S}_-$, and $\mathbf{S}_z$ are the cooperative pseudospin operators obeying commutation relations:

$$[\mathbf{S}_+,\mathbf{S}_-]=2\mathbf{S}_z,[\mathbf{S}_z,\mathbf{S}_+]=\mathbf{S}_+,\quad [\mathbf{S}_z,\mathbf{S}_-]=-\mathbf{S}_-, \tag{3.2}$$

and, finally, the unit system is used where both the Planck constant and the speed of light are set to one.

To make the model Hamiltonian time periodic, we turn to the rotating frame by applying unitary transform $\mathbf{R}(t)=\exp[-i\Omega(\mathbf{S}_z+\mathbf{a}^\dagger\cdot\mathbf{a})t]$. The model Hamiltonian and the other operators of the system are transformed here in the following manner:

$$\mathbf{H}'(t)=\mathbf{R}^\dagger(t)\cdot\mathbf{H}(t)\cdot\mathbf{R}(t)-i\,\mathbf{R}^\dagger(t)\cdot\frac{d}{dt}\mathbf{R}(t),$$
$$\mathbf{A}'(t)=\mathbf{R}^\dagger(t)\cdot\mathbf{A}\cdot\mathbf{R}(t), \tag{3.3}$$

where $\mathbf{A}$ stands for each operator of the system. This yields the time periodic Hamiltonian

$$\mathbf{H}(t)'=(\omega_0-\Omega)\mathbf{S}_z'+(\omega-\Omega)\mathbf{a}^{\dagger'}\cdot\mathbf{a}'+g(t)\mathbf{S}_+'+g^*(t)\mathbf{S}_-'+\kappa_{aq}(\mathbf{S}_+'\cdot\mathbf{a}'+\mathbf{S}_-'\cdot\mathbf{a}^{\dagger'}). \tag{3.4}$$

In Eqs. (3.3) and (3.4), the primes are used to label operators in the rotating frame. It is conventional, however, to use the same notations for operators in all the time representations. For this reason we drop the primes hereafter.

The next step in our paper is to present the model Hamiltonian (3.4) as a sum of the zeroth-order Hamiltonian and the interaction Hamiltonian. Assuming coupling constant κ_q to be small compared to both the modulation frequency and the strength of the polychromatic field, $\max(|g(t)|)$, we set

$$\mathbf{H_0}(t)=\mathbf{H_{0a}}(t)+\mathbf{H_{0f}}, \tag{3.5}$$

$$\mathbf{H_{0a}}(t)=(\omega_0-\Omega)\mathbf{S}_z+g(t)\mathbf{S}_+ +g^*(t)\mathbf{S}_-, \tag{3.6}$$

$$\mathbf{H_{0f}}=(\omega-\Omega)\mathbf{a}^\dagger\cdot\mathbf{a}, \tag{3.7}$$

$$\mathbf{V}(t)=\kappa_{\mathrm{fq}}(\mathbf{S}_+\cdot\mathbf{a}+\mathbf{S}_-\cdot\mathbf{a}^\dagger). \tag{3.8}$$

The zeroth-order Hamiltonian is a sum of the two commutative operators: the time-periodic Hamiltonian of the dressed atom $\mathbf{H_{0a}}(t)$, and that of the quantized mode $\mathbf{H_{0f}}$. The time-periodic field strength $g(t)$ may be represented as follows:

$$g(t)=g_0+\tilde{g}(t);\qquad g_0=\mathbf{M}\{g\};\quad \mathbf{M}\{\tilde{g}\}=0, \tag{2.26}$$

where g_0 is the amplitude of the field component oscillating at the carrier frequency Ω, while function $\tilde{g}(t)$ is the remaining part of the driving field oscillating at frequencies other than Ω. Assuming the carrier frequency to coincide with the atomic transition ($\Omega=\omega_0$), one solves the zeroth-order Schrödinger equation to yield

$$\mathbf{Q_0}=(\omega-\Omega)\mathbf{a}^\dagger\cdot\mathbf{a}+g_0(\mathbf{S}_+ +\mathbf{S}_-),$$
$$\mathbf{u_0}(t)=\cos[G(t)]\mathbf{I}-i\sin[G(t)](\mathbf{S}_+ +\mathbf{S}_-), \tag{3.10}$$

where $G(t)=\int_0^t\tilde{g}(t')dt'$ is a time-periodic function.

For the sake of simplicity, we consider below the case of pure resonance only, where $\omega=\omega_0=\Omega$. If this is the case, one may set amplitude g_0 to zero without limiting the generality of the analysis. Actually, if $\omega=\Omega$ term $g_0\mathbf{S}_+ +g_0^*\mathbf{S}_-$ is eliminated from Hamiltonian (3.4) by applying unitary transform $\mathbf{D}(-g_0/\kappa_{aq})$, where $\mathbf{D}(\alpha)$ is the shift operator given by $\mathbf{D}(\alpha)=\exp(\alpha\mathbf{a}^\dagger-\alpha^*\mathbf{a})$ [20]. Physically, the transform mentioned above moves the field component at frequency Ω from the driving field to the quantized mode without changing the actual dynamics of the system. For this reason, we assume hereafter that $g_0=0$ and, therefore, $\mathbf{Q_0}=\mathbf{0}$. Moreover, we consider here the case of a single atom called the dressed-atom Jaynes-Cummings model (DAJCM) (see [17] and [18]) where pseudospin operators $\mathbf{S}_+$ and $\mathbf{S}_-$ obey relations

$$\mathbf{S}_+\cdot\mathbf{S}_-+\mathbf{S}_-\cdot\mathbf{S}_+=\mathbf{I};\qquad (\mathbf{S}_+)^2=(\mathbf{S}_-)^2=\mathbf{0}. \tag{3.11}$$

Using unitary transform $\mathbf{u}_0(t)$ to convert the interaction term (3.8) to the time-periodic picture one gets

$$\mathbf{V_{TP}}(t)=\kappa_{\mathrm{fq}}\left\{\mathbf{S}_x+i\cos[2G(t)]\mathbf{S}_y-\frac{i}{2}\sin[2G(t)]\mathbf{S}_z\right\}\cdot\mathbf{a}+\mathrm{H.c.}, \tag{3.12}$$

where $\mathbf{S}_x=(\mathbf{S}_+ +\mathbf{S}_-)/2$, $\mathbf{S}_y=(\mathbf{S}_+ -\mathbf{S}_-)/(2i)$, and H.c. stands for Hermitian conjugation. The first-order quasienergy operator is then obtained from Eq. (2.13) assuming $\mathbf{Q_0}=\mathbf{0}$, $\tilde{\mathbf{W}}(t)=\mathbf{W_0}(t)=\mathbf{I}$. In this way one gets

$$\mathbf{Q}_1=\mathbf{M}\{\mathbf{V_{TP}}\}=\kappa_{\mathrm{fq}}\left\{\mathbf{S}_x+i\psi_1\mathbf{S}_y-\frac{i}{2}\psi_2\mathbf{S}_z\right\}\cdot\mathbf{a}+\mathrm{H.c.}, \tag{3.13}$$

where $\psi_1=\mathbf{M}\{\cos[2G(t)]\}$ and $\psi_2=\mathbf{M}\{\sin[2G(t)]\}$. The first-order quasienergy operator above coincides with the effective Hamiltonian obtained in [17] using the other approach. The spectrum of this Hamiltonian is calculated, in its turn, in Ref. [18].

Let us focus on a particular case where the driving field is bichromatic. More precisely, we set $g(t)=\sigma\omega_{\mathrm{M}}\sin(\omega_{\mathrm{M}}t)$, where σ is the scaled amplitude of the driving field assumed to be much greater than the scaled coupling constant, $\kappa\equiv\kappa_{\mathrm{fq}}/\omega_{\mathrm{M}}$. This yields $\psi_1=J_0(2\sigma)$ and $\psi_2=0$. Based on Ref. [18], the eigenvalues of the first-order quasienergy operator are

$$E_0=0;\quad E_{\pm n}=\pm\omega_{\mathrm{M}}\kappa\sqrt{|D|n},\qquad n=1,2,\ldots, \tag{3.14}$$

where D is the numeric parameter called the DAJCM discriminant. The discriminant above depends on the strength of the driving field. The particular values of the field strength where $D=0$ are referred to here as the singular points. At these points, the quasienergy spectrum $\{E_n : n=0,\pm 1, \pm 2, \ldots,\}$ becomes continuous while the eigenvectors gain infinite norm. The discriminant of quasienergy operator $\mathbf{Q}_1$ is $D=\mathrm{J}_0(2\sigma)$ and, therefore, the singular points are the zeros of the Bessel function.

Based on the formalism of Ref. [18] the eigenvectors of quasienergy operator $\mathbf{Q}_1$ in case of the bichromatic driving field are obtained from those of the conventional JCM Hamiltonian by applying squeeze operator $\mathbf{S}(r)=\exp([r^*\mathbf{a}^2 - r(\mathbf{a}^\dagger)^2]/2)$ to yield

$$|\psi_0\rangle=\mathbf{S}(r)|\psi_0\rangle_{\mathrm{JCM}}=|0;r\rangle|\theta_1\rangle,$$
$$|\psi_{\pm n}\rangle=\mathbf{S}(r)|\psi_{\pm n}\rangle_{\mathrm{JCM}}=(1/\sqrt{2})(|n;r\rangle|\theta_0\rangle\pm i|n-1;r\rangle|\theta_1\rangle), \tag{3.15}$$

where the squeeze parameter is given by

$$r=-\ln(\sqrt{|\mathrm{J}_0(2\sigma)|}). \tag{3.16}$$

Here, $|\theta_0\rangle$ and $|\theta_1\rangle$ are the eigenvectors of operator $\mathbf{S}_z$ in the time-periodic representation called the quasienergy states or the Floquet states as well and vectors $|n;r\rangle=\mathbf{S}(r)|n\rangle$ are the squeezed number states of the quantized mode. Note that $|0;r\rangle=\mathbf{S}(r)|0\rangle$ is the conventional squeezed vacuum state.

The quasienergy operator $\mathbf{Q}$ calculated to an arbitrary order of the perturbation theory may be represented as

$$\mathbf{Q}=\mathbf{L}\cdot\mathbf{Q}_{\mathrm{E}}\cdot\mathbf{L}^\dagger, \tag{3.17}$$

where operator $\mathbf{Q}_{\mathrm{E}}$ includes the odd-order perturbations only. The unitary transform $\mathbf{L}$ is given by

$$\mathbf{L}=\exp(i\sqrt{2}\kappa\mathbf{x}\cdot\mathbf{S}_z f_1)\exp(-i\kappa^2(\mathbf{p}\cdot\mathbf{x}+\mathbf{x}\cdot\mathbf{p})\cdot\mathbf{S}_z f_2), \tag{3.18}$$

with $\mathbf{x}=i(\mathbf{a}-\mathbf{a}^\dagger)/\sqrt{2}$ and $\mathbf{p}=(\mathbf{a}+\mathbf{a}^\dagger)/\sqrt{2}$ being the effective coordinate and the effective momentum of the quantized field, respectively. Numeric parameters f_1 and f_2 depend on the strength of the driving field. We do not issue the cumbersome relations for these parameters here since the eigenvalue spectrum of the quasienergy operator does not depend on f_1 and f_2.

Apparently, the eigenvalue spectrum of the reduced quasienergy operator $\mathbf{Q}_{\mathrm{E}}$ is the same as that of the quasienergy operator $\mathbf{Q}$. In the framework of the third-order perturbation theory operator, $\mathbf{Q}_{\mathrm{E}}$ assumes the form

$$\mathbf{Q_E}=\mathbf{Q}_1+\mathbf{Q_{E3}},$$
$$\mathbf{Q_{E3}}=\omega_M\sqrt{2}\kappa^3\left(\mathbf{x}\cdot\mathbf{p}\cdot\mathbf{x}\cdot\mathbf{S_x}F_1(\sigma)-\tfrac{1}{2}\mathbf{x}^3\cdot\mathbf{S_y}F_2(\sigma)\right), \tag{3.19}$$

where

$$F_1(\sigma)=-2\sum_{k=1}^{\infty}\left(\frac{\mathrm{J}_k(2\sigma)}{k}\right)^2,$$

$$F_2(\sigma)=2\sum_{k,k'=-\infty}^{\infty}\frac{\mathrm{J}_{2k'+1}(2\sigma)\mathrm{J}_{2k+1}(2\sigma)\mathrm{J}_{2k+2k'+2}(2\sigma)}{(2k+1)(2k'+1)}$$
$$-\frac{1}{2}\sum_{\substack{k,k'=-\infty\\ k,k',k+k'\neq 0}}^{\infty}\frac{\mathrm{J}_{2k'}(2\sigma)\mathrm{J}_{2k}(2\sigma)\mathrm{J}_{2k+2k'}(2\sigma)}{2k2k'},$$

with $\mathrm{J}_k(2\sigma)=(-1)^k\mathrm{J}_{-k}(2\sigma)$.

For $x\ll 1$, one may set $\mathbf{Q}_E\approx\mathbf{Q}_1$. The corresponding eigenvalues given by Eq. (3.14) may be attributed therefore to the central potential well centered at $x=0$. There are two other potential wells settled symmetrically around the central one and referred to here as the side wells. To reveal the presence of the side wells, let us transform operator $\mathbf{Q}_E$ in the following manner: $\mathbf{Q}'_E=\exp(ix_0\mathbf{p})\mathbf{Q}_E\exp(-ix_0\mathbf{p})$ with x_0 being a real number. It is worth noting that $\exp(ix_0\mathbf{p})$ is the unitary shift operator obeying relation $\exp(ix_0\mathbf{p})\mathbf{x}\exp(-ix_0\mathbf{p})=\mathbf{x}+x_0$. Parameter x_0 should be chosen here to eliminate the pure atomic term in $\mathbf{Q}'_E$ which does not depend on both $\mathbf{x}$ and $\mathbf{p}$. This yields the following expression determining the location of the side dips related to the central one:

$$x_0=\pm\sqrt{2\mathrm{J}_0(2\sigma)/[\kappa^2F_2(\sigma)]}. \tag{3.20}$$

It is assumed here that 2σ does not exceed the first zero of the Bessel function, $\mathrm{J}_0(2\sigma)$.

To find the approximate expressions for the quasienergy spectrum of the side dips, one may linearize operator $\mathbf{Q}'_E$ with respect to $\mathbf{x}$ yielding

$$\mathbf{Q}_{\mathrm{E}}^{\mathrm{lin}}=\sqrt{2}\omega_{\mathrm{M}}\kappa[\mathbf{p}\,\mathbf{S}_x\mathrm{J}(2\sigma)-2\,\mathbf{x}\,\mathbf{S}_y\mathrm{J}_0(2\sigma)], \tag{3.21}$$

where $\mathrm{J}(2\sigma)\equiv 1+2F_1(\sigma)\mathrm{J}_0(2\sigma)/F_2(\sigma)$. Similarly to the first-order quasienergy operator $\mathbf{Q}_1$, the linearized third-order quasienergy operator $\mathbf{Q}_{\mathrm{E}}^{\mathrm{lin}}$ is the bilinear combination of the atomic pseudospin operators and the photon annihilation and creation operators. The formalism of Ref. [18] may be applied, therefore, to find the eigenvalues of operator $\mathbf{Q}_{\mathrm{E}}^{\mathrm{lin}}$ yielding

$$E_{\pm n}^{\mathrm{lin}}=\pm\omega_{\mathrm{M}}\kappa\sqrt{D'n},\quad n=0,1,\ldots, \tag{3.22}$$

with the discriminant given by $D'=2J_0(2\sigma)J(2\sigma)$. The eigenvectors of this operator may be expressed here in terms of the shifted squeezed number states of the quantized mode $|n;r';x_0\rangle\equiv\exp(-ix_0p)|n;r'\rangle$ with the squeeze parameter determined by: $\exp(-2r')=J(2\sigma)/[2\,J_0(2\sigma)]$. Using the formalism of Ref. [18] one gets [compare with Eq. (3.15)]

$$|\psi'_0\rangle=|0;r';x_0\rangle|\theta_1\rangle,$$
$$|\psi'_{\pm n}\rangle=(1/\sqrt{2})(|n;r';x_0\rangle|\theta_0\rangle\pm i|n-1;r';x_0\rangle|\theta_1\rangle). \tag{3.23}$$

It appears, therefore, that the spectrum of the quasienergy operator includes three series of eigenvalues corresponding to three potential wells: the central well and the side ones as well. Here, the term ''potential well'' refers to the domain of x values where the generalized JCM Hamiltonian considered

in Ref. [18] may approximate the quasienergy operator of the system in question. Apparently, if the distance between the side wells determined by Eq. (3.20) is large enough, the eigenvalues (3.22) are doubly degenerate. However, bringing together the side wells should remove the degeneracy through the barrier tunneling effect. This means that the quasienergy levels of the side wells should split into doublets at certain values of field strength, σ. The results of the perturbation approach, including the quasilevel splitting effect, are proved below using the precise numerical solution of the time-dependent Schrödinger equation.

Apparently, the conclusion that three wells are only present comes from using the third-order perturbation theory. Including higher-order perturbations may increase the number of wells. However, to reach a well of high order, one needs a significant number of photons to be present in the quantized mode. It seems, therefore, that the wells of a low order are only relevant to the up-to-date QED experiments.

The accuracy of the analytical theory above can hardly be evaluated. For this reason, we present the comparison of the analytical results and the straightforward numeric computations below.

IV. QUASILEVEL DIAGRAM OF THE BICHROMATICALLY DRIVEN DAJCM

We used the sparse matrix technique of MATLAB 6 to calculate the quasienergy spectrum of the bichromatically driven DAJCM. The calculations were organized in the following order: First, we applied the fourth-order Runge-Kutta method for solving the matrix differential equation for the time-evolution operator:

$$\frac{d}{d\,t}\mathbf{W}(t) = -i\mathbf{V}_{\mathrm{TP}}(t)\cdot\mathbf{W}(t), \tag{4.1}$$

with initial condition $\mathbf{W}(0)=\mathbf{I}$. Here, $\mathbf{W}(t)$ is the time evolution operator, and $\mathbf{V}_{\mathrm{TP}}(t)$ is the time-periodic perturbation Hamiltonian with period $T_{\mathrm{M}}=2\pi/\omega_{\mathrm{M}}$ given by Eq. (3.12). The driving field was implied bichromatic and, therefore, we set $G(t)=\sigma\sin(\omega_{\mathrm{M}}t)$. We used the matrix representation of operators $\mathbf{W}(t)$ and $\mathbf{V}_{\mathrm{TP}}(t)$ in the basis of product states $|n\rangle|\theta_0\rangle$ and $|n\rangle|\theta_1\rangle$ where $n=0,1,2,\ldots,$. The representation was truncated at $n=n_{\max}$. The maximum number of photons $n_{\max}$ was chosen here to calculate all the quasienergy levels of interest with a sufficient accuracy. Practically, the numeric results were obtained for $n_{\max}=60-130$. Equation (4.1) was solved for matrix $\mathbf{W}(t)$ within the time domain $0\leqslant t\leqslant T_{\mathrm{M}}$ to yield the monodromy matrix $\mathbf{M}=\mathbf{W}(T_{\mathrm{M}})$ [19]. Then, given the monodromy matrix, the quasienergy operator $\mathbf{Q}$ is determined by the relation [19] $\mathbf{M}=\exp(-i\,\mathbf{Q}\,T_{\mathrm{M}})$. At the final step of our calculations, the eigenvalues E_{n} of the quasienergy operator were evaluated numerically and put in the ascending order.

Figure 1 presents the quasienergy diagram obtained in this way for $\kappa=0.1$. To get the reliable results, the calculations were repeated several times for various values of $n_{\max}$. It was found that the sufficient accuracy was reached for $n_{\max}=70$. The additional plots 1–4 crossing the horizontal axes at

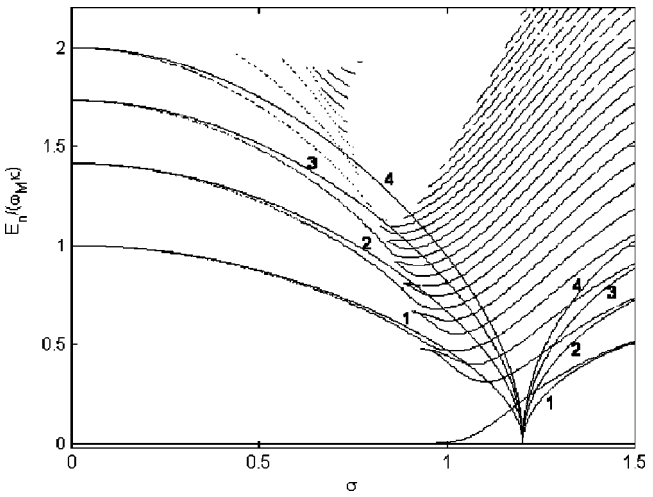

FIG. 1. Quasilevel diagram of the bichromatically driven DAJCM. Quasilevels 1 – 4 are obtained by Eq. (3.14) assuming $D=J_0(2\cdot\sigma)$ and correspond to the limiting case of infinitesimal κ. The other quasilevels are obtained for $\kappa=0.1$ using the numeric technique described in Sec. IV.

the singular point are the approximated (first-order) quasienergy values of the central potential well given by Eq. (3.14) with $D=J_0(2\sigma)$. Far from the singular point, the approximated quasienergy values come close to those calculated numerically.

The quasienergy levels undergoing double splitting at certain values of the driving field strength σ are attributed to the side potential wells. More detailed diagrams of these quasienergy levels are presented in Figs. 2(a) and 2(b). In this figure, the solid plots are calculated using the numeric technique above for $n_{\max}=125$. Simultaneously, the dashed plots obtained within the third-order perturbation theory show the eigenvalues of quasienergy operator $\boldsymbol{Q}_{\mathrm{E}}$ given by Eq. (3.19). In case $\kappa=0.05$ [Fig. 2(a)], the third-order perturbation theory describes the splitting of the quasienergy levels due to the tunneling effect with rather good accuracy. For $\kappa=0.1$ [Fig. 2(b)], the third-order calculations yield appreciable errors yet exhibiting the qualitative agreement with the numeric results.

V. SQUEEZING AND NONADIABATIC TRANSITIONS IN THE BICHROMATICALLY DRIVEN DAJCM

This section discusses a possible way of obtaining a high squeezing degree in one of the field quadratures. The consideration is restricted to the case of the bichromatic driving field with the function of modulation given by $g(t)=\sigma\omega_{\mathrm{M}}\sin(\omega_{\mathrm{M}}t)$.

It is seen from Eq. (3.15) that eigenvector $|\psi_0\rangle$ of the first-order quasienergy operator includes the squeezed vacuum $|0,r\rangle$ of the cavity field. The squeeze parameter r is obtained here from Eq. (3.16). Within the first-order approximation, the squeeze parameter becomes infinitely large when 2σ tends to the first zero of the Bessel function, $J_0(2\sigma)$. To get a large degree of squeezing, one may start, therefore, from the situation where the driving field is off, the cavity

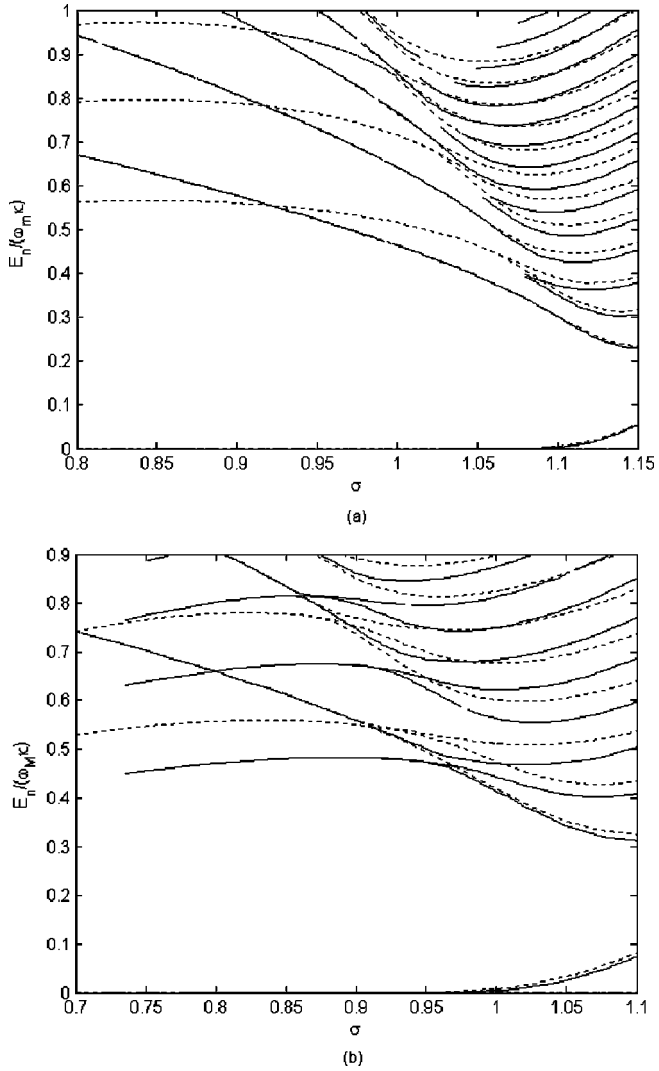

FIG. 2. Fragments of the quasilevel diagram for $\kappa=0.05$ (a) and 0.1 (b) exhibiting the quasilevel splitting effect. The solid plots present the precise numeric results. The dashed plots are the eigenvalues of the third-order quasienergy operator $\mathbf{Q}_{\mathrm{E}}$ given by Eq. (3.19).

field is in the vacuum state $|0\rangle$, and the TLA is in the upper energy state $|1\rangle$. This means that the DAJCM is initially at the quasienergy level E_0 with the zero value of the squeeze parameter. Then, the driving field amplitude σ should grow slowly until $\mathrm{J}_0(2\sigma)$ becomes zero. At the same time, the squeeze parameter should reach its maximum value.

Using the procedure above, the maximum attainable degree of squeezing is limited by the two unavoidable effects. First, the higher-order terms of the quasienergy operator may cause additional fluctuations of the cavity field. Second, the system may skip nonadiabatically from quasienergy level E_0 to the other quasienergy levels [22]. The skipping probability increases here near the singular point where the quasienergy levels come close to each other.

To study the dynamics of the bichromatically driven DAJCM at the slow increase of the driving field amplitude σ we solved the Schrödinger equation with Hamiltonian (3.4) numerically assuming $g(t)=\sigma(t)\omega_{\mathrm{M}}\sin(\omega_{\mathrm{M}}t)$. The technique for solving the atom-field Schrödinger equation and its software implementation were similar to those described in the previous section. At the final step of the calculations we evaluated the standard deviation ΔX_1 of cavity field quadrature $\mathbf{X}_1=(\mathbf{a}+\mathbf{a}^{\dagger})/2$. It is worth noting here that the squeezing occurs provided $\Delta X_1 \leqslant 0.5$ [20].

The alternative way of describing the nonadiabatic transitions between the quasienergy states is to include a special Hamiltonian proportional to $\dot{\sigma}(t)$. This Hamiltonian called hereon the nonadiabatic Hamiltonian may be derived as explained below.

It follows from Eqs. (3.13)–(3.15) that the first-order quasienergy operator of the bichromatically driven DAJCM, $\mathbf{Q_1}=\omega_M\kappa[\mathbf{S_x}+iJ_0(2\sigma)\mathbf{S_y}]\cdot\mathbf{a}+\mathrm{H.c.}$, can be represented as $\mathbf{Q_1}=\sqrt{J_0(2\sigma)}\mathbf{S}(r(\sigma))\mathbf{H}_{\mathrm{JCM}}\mathbf{S}^{\dagger}(r(\sigma))$, where $\mathbf{H}_{\mathrm{JCM}}=\omega_M\kappa(\mathbf{S_x}+i\mathbf{S_y})\cdot\mathbf{a}+\mathrm{H.c.}$ is the conventional JCM Hamiltonian and $\mathbf{S}(r)=\exp([r^*\mathbf{a}^2-r(\mathbf{a}^{\dagger})^2]/2)$ is the squeeze operator with the squeeze parameter r given by relation (3.16). Neglecting the fast oscillations at the multiples of the modulation frequency, the first-order Schrödinger equation is

$$i\frac{d}{dt}|\psi\rangle=\mathbf{Q_1}[\sigma(t)]|\psi\rangle. \tag{5.1}$$

One may describe the nonadiabatic time evolution in the explicit manner using the following change of time representation

$$|\tilde{\psi}(t)\rangle=\mathbf{S}^{\dagger}[r(\sigma(t))]|\psi(t)\rangle. \tag{5.2}$$

Actually, applying transform (5.2), the Schrödinger equation becomes

$$i\frac{d}{dt}|\tilde{\psi}\rangle=[\sqrt{J_0(2\sigma)}\mathbf{H}_{\mathrm{JCM}}+\mathbf{H}_{\mathrm{non}}]|\tilde{\psi}\rangle, \tag{5.3}$$

with the nonadiabatic Hamiltonian given by

$$\mathbf{H}_{\mathrm{non}}=-\frac{i}{2}\frac{d\sigma}{dt}[\mathbf{a}^2-(\mathbf{a}^{\dagger})^2]\left|\frac{J_1(2\sigma)}{J_0(2\sigma)}\right|. \tag{5.4}$$

The first term in Eq. (5.3) describes the adiabatic time evolution of the DAJCM. Given by this type of time evolution the probability of disclosing the system at any quasienergy level, $E_{\pm n}$, $n=0,1,2\ldots$, is held fixed in time while the phases of the corresponding wave functions change. On the contrary, Hamiltonian $\mathbf{H}_{\mathrm{non}}$ enforces transitions among the quasienergy states with the transition rate being proportional to the first-time derivative of the driving field amplitude. It should be emphasised that expression (5.4) for the nonadiabatic Hamiltonian is valid for the first-order perturbation theory only. Therefore, it becomes inapplicable just near the singular points where the denominator, $|\mathrm{J}_0(2\sigma)|$, becomes small. Simultaneously, the numeric results are always available by solving the Schrödinger equation with time-dependent Hamiltonian (3.4) using a Runge-Kutta method. The latter calculations are rather time consuming. Actually, the time step should be chosen much shorter than

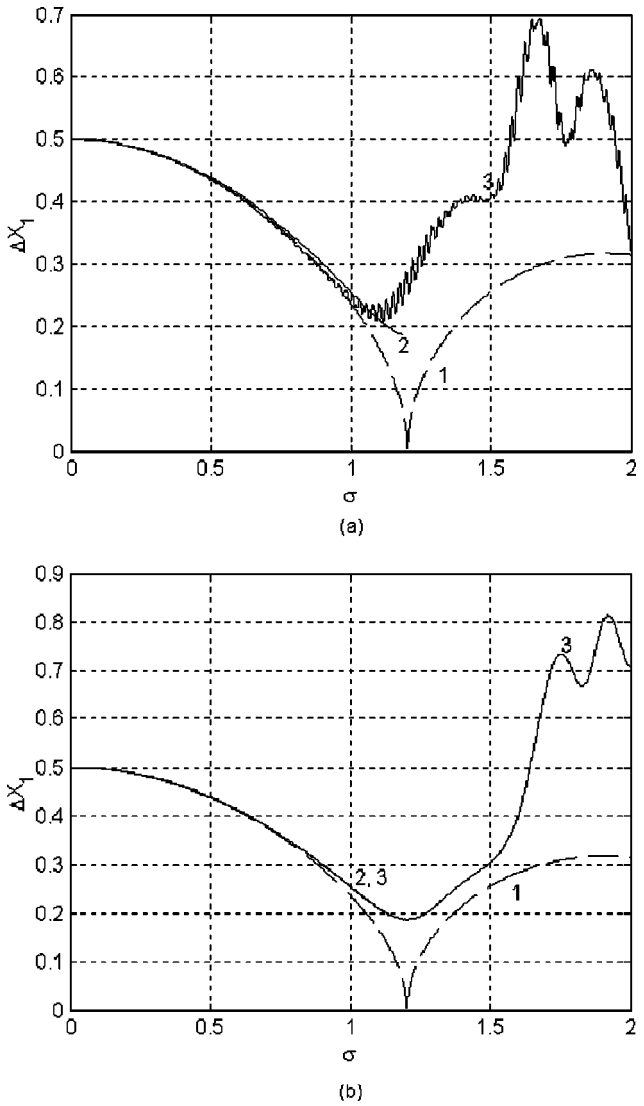

FIG. 3. The standard deviation of quadrature $\mathbf{X}_1$ vs the scaled amplitude of the driving field for $\sigma=0.05\times\omega_M\times\kappa\times t$, with $\kappa=0.15$ (a) and $\kappa=0.005$ (b). Plot 1 is obtained within the first-order perturbation theory dropping the nonadiabatic transitions, plot 2 allows for the nonadiabatic transitions but still uses the first-order perturbation theory, and plot 3 presents the precise numeric solution for the time-dependent Schrödinger equation.

the modulation period while the simulation should cover a long time interval where σ changes from zero to the singular point.

Let us turn to the calculation results. In Figs. 3 and 4, the TLA is initially in the upper-state one while the cavity field starts its time evolution from the vacuum state. Therefore, the system is initially at the quasienergy level E_0 while both the driving field amplitude and the squeeze parameter are zero. Figure 3 shows the standard deviation of quadrature $\mathbf{X}_1$ against amplitude σ when the amplitude grows linearly in time: $\sigma=0.05\omega_M\kappa t$, with $\kappa=0.15$ (a) and $\kappa=0.005$ (b). Plot 1 is calculated using relation $\Delta X_1=0.5\exp[-r(\sigma)]$, where the squeeze parameter is given by Eq. (3.16). Hence, this plot neglects the effect of the higher-order perturbations and that of the nonadiabatic transitions either exhibiting the infinitely large squeezing at the singular point. Plot 2 is obtained by using the nonadiabatic Hamiltonian as described above. This approach allows for the nonadiabatic transitions but yet it neglects the perturbations of order more than one. Therefore, it becomes invalid just near the singular point where we interrupt plot 2. Finally, plot 3 presents the precise numeric solution of the Schrödinger equation with Hamiltonian (3.4) as explained above.

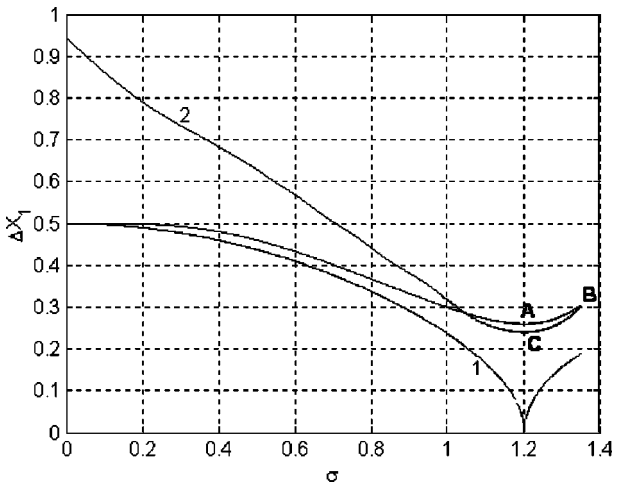

FIG. 4. The standard deviation of quadrature $\mathbf{X}_1$ vs the scaled amplitude of the driving field for $\sigma=1.35\times\sin(0.2\times\omega_M\times\kappa\times t/1.35)$ and $\kappa=0.005$. Plot 1 is the same as in Fig. 3; plot 2 ($ABCD$) is the precise numeric solution for the time-dependent Schrödinger equation.

It appears that for the sufficiently small coupling constant, $\kappa\approx0.005$, the first-order perturbation theory gives rather precise results. Actually, one finds no appreciable distinction between lines 2 and 3 in Fig. 3(b). Furthermore, fast oscillations at frequency ω_{M} are still present for $\kappa=0.15$ [Fig. 3(a)] but they fully smooth out for $\kappa=0.005$ [Fig. 3(b)]. However, the maximum attainable degree of squeezing does not increase significantly when switching the coupling constant κ from 0.15 to 0.005.

In order to enhance squeezing of the cavity field, one may try to cross the singular point several times in alternating directions. However, Fig. 4 suggests that the effect of the second crossing should be rather small because the first crossing perturbs the system so that it skips level E_0 with a significant probability.

VI. CONCLUSION

We have developed a perturbation technique to derive the quasienergy operator of the dressed-atom Jaynes-Cummings model (DAJCM), the latter being the dipole-coupled system of a polychromatically driven atom and a cavity mode. The eigenvectors of the first-order quasienergy operator include the squeezed number states of the cavity mode. At certain values of the driving field amplitude called the singular points, the squeezing degree becomes infinitely large while the eigenvalues of the quasienergy operator come together to form the continuous spectrum. The infinite values are removed by allowing for the perturbations of order more than one. Simultaneously, the additional eigenvalues appear. All

the eigenvalues obtained within the third-order perturbation technique may be attributed hereby to three potential wells with the eigenvalues of the central well corresponding to the first-order quasienergy operator. The doubly degenerated eigenvalues of the side wells correspond to the third-order term in the perturbation expansion of the quasienergy operator. At certain values of the driving field amplitude, the side wells come sufficiently close to the central one to remove the degeneracy. This results in double splitting of the corresponding quasienergy levels.

In addition to the approximated analytical theory, we have developed the numerical technique for calculating the eigenvalue spectrum of the quasienergy operator. It appeared that the numerical and analytical results exhibit quantitative agreement. The calculated quasienergy levels undergo splitting and avoided crossing when the amplitude of the driving field approaches the singular points.

A possible way of squeezing a cavity field quadrature consists of tempering the amplitude of the driving field towards a singular point. In this respect, there are two unavoidable effects that limit the maximum attainable squeezing degree, specifically, the nonadiabatic transitions among the quasienergy levels and terms of order three and higher in the perturbative expansion of the quasienergy operator. Both effects gain special significance near the singular points. The former effect may be described by embedding the additional term in the first-order Schrödinger equation. Being proportional to the first-time derivative of the driving field amplitude, this term is called the nonadiabatic Hamiltonian.

We used the precise numerical solution of the time-dependent Schrödinger equation, and the first-order perturbation technique with nonadiabatic Hamiltonian as well, to analyze the limitations of the attainable squeezing degree. To enhance squeezing, one may cross the singular point several times in alternating directions. It appears, however, that the nonadiabatic effect perturbs significantly the quantum state of the system at the first crossing. Consequently, the additional squeezing in time of the subsequent crossings reduces or becomes fully eliminated.

[1] P. Meystre and M. Sargent III, *Elements of Quantum Optics* (Springer, Berlin, 1998).

[2] *Cavity Quantum Electrodynamics*, Advances in Atomic, Molecular and Optical Physics Series, Supplement 2, edited by P. R. Berman (Academic Press, Boston, 1994).

[3] D. Meschede, H. Walther, and G. Muller, Phys. Rev. Lett. **54**, 551 (1985); G.M. Meyer, M. Loffler, and H. Walther, Phys. Rev. A **56**, R1099 (1997).

[4] R.J. Thompson, G. Rempe, and H.J. Kimble, Phys. Rev. Lett. **68**, 1132 (1992).

[5] G. Rempe, H. Walther, and N. Klein, Phys. Rev. Lett. **58**, 353 (1987).

[6] E.T. Jaynes and F.W. Cummings, Proc. IEEE **51**, 89 (1963).

[7] M. Tavis and F.W. Cummings, Phys. Rev. **170**, 379 (1968).

[8] P. Meystre, E. Geneux, A. Quattrapani, and A. Faist, Nuovo Cimento Soc. Ital. Fis., B **25**, 21 (1975); P. Meystre and M.S. Zubairy, Phys. Lett. A **89**, 390 (1982); M.H. Mahran, Phys. Rev. A **45**, 5113 (1992).

[9] B. Yurke, W. Schleich, and D.F. Walls, Phys. Rev. A **42**, 1703 (1990).

[10] P. Filipowicz, J. Javanainen, and P. Meystre, Opt. Commun. **58**, 327 (1986).

[11] C.A. Blockley, D.F. Walls, and H. Risken, Europhys. Lett. **17**, 509 (1992).

[12] Shi-Biao Zheng, Phys. Lett. A **245**, 11 (1998); Xueli Luo, Xiwen Zhu, and Ying Wu, *ibid.* **237**, 354 (1998).

[13] A. Sinatra, J.F. Roch, K. Vigneron, P. Grelu, J.P. Poizat, K. Wang, and P. Grangier, Phys. Rev. A **57**, 2980 (1998).

[14] K. Vogel, V.M. Akulin, and W.P. Schleich, Phys. Rev. Lett. **71**, 1816 (1993).

[15] H. Nha, Y.-T. Chough, and K. An, Phys. Rev. A **62**, 021801(R) (2000).

[16] P. Alsing, D.-S. Guo, and H.J. Carmichael, Phys. Rev. A **45**, 5135 (1992).

[17] M.Z. Smirnov, Zh. Éksp. Teor. Fiz. **112**, 819 (1997) [Sov. Phys. JETP **85**, 441 (1997)]; **114**, 474 (1998) [**87**, 260 (1998)]; Quantum Semiclassic. Opt. **10**, 765 (1998); Quantum Electron. **30**, 821 (2000).

[18] G.P. Miroshnichenko and M.Z. Smirnov, Opt. Commun. **182**, 393 (2000).

[19] V.A. Yakubovich and V. M. Starzhinskii, *Linear Differential Equations with Periodic Coefficients* (Wiley, New York, 1975), Vol. I and II.

[20] H.P. Yuen, Phys. Rev. A **13**, 2226 (1976); G.J. Milburn and D.F. Walls, Opt. Commun. **39**, 401 (1981).

[21] A.H. Nayfeh, *Introduction to Perturbation Techniques* (Wiley, New York, 1981), Sec. 11.

[22] P.A. Braun and G.P. Miroshnichenko, Zh. Éksp. Teor. Fiz. **80**, 68 (1981) [Sov. Phys. JETP **54**, 27 (1981)]; P.A. Braun and G.P. Miroshnichenko, Opt. Spectrosk. **45**, 863 (1978), [Opt. Spectrosc. **45**, 863 (1978)].